DOI:
10.2217/nnm-2018-0289

Asenapine maleate loaded nanostructured lipid carriers: Optimization and *in vitro, ex vivo* and *in vivo* evaluations

Renuka Suresh Managuli[a], Julie Tzu-Wen Wang[b], Farid N. Muhammad Faruqu[b], Varun Kushwah[c], Sushil Y. Raut[a], A. B. Shreya[a], Khuloud T. Al-Jamal[b], Sanyog Jain[c], Srinivas Mutalik[a]*

[a] Department of Pharmaceutics, Manipal College of Pharmaceutical Sciences, Manipal Academy of Higher Education, Manipal 576104, Karnataka State, India

[b] School of Cancer and Pharmaceutical Sciences, Faculty of Life Sciences & Medicine, King's College London, London SE1 9NH, UK

[c] Centre for Pharmaceutical Nanotechnology, Department of Pharmaceutics, National Institute of Pharmaceutical Education and Research, Sector 67, S.A.S. Nagar (Mohali), Punjab 160062, India

*** For correspondence:**
Dr. Srinivas Mutalik
Department of Pharmaceutics
Manipal College of Pharmaceutical Sciences
Manipal Academy of Higher Education, Manipal 576104
Karnataka State, India
Email: ss.mutalik@manipal.edu
Phone: +91-820-2922482
Fax: +91-820-2571998

ABSTRACT

Aim: To prepare nanostructured lipid carriers (NLCs) loaded with asenapine maleate (ASPM) to increase its oral bioavailability by intestinal lymphatic uptake. **Materials & Methods:** ASPM-NLCs were prepared by ultrasound dispersion technique by adopting Design of Experiment (DoE) approach and characterized. **Results:** The optimized formulation exhibited good physicochemical parameters. DSC and XRD studies indicated the amorphized nature of ASPM in lipid matrix. *In vitro* drug release study indicated the sustained release of drug from NLCs. ASPM-NLCs showed greater permeability across Caco2 cells and everted rat ileum. ASPM-NLCs showed greater cellular uptake, superior preclinical oral bioavailability and higher efficacy in reducing the L-DOPA-carbidopa induced locomotor count compared to plain drug. **Conclusion:** ASPM-NLCs were successfully developed which showed enhanced performance both *in vitro* and *in vivo.*

Keywords: Asenapine maleate, Nanostructured lipid carriers, Caco 2 cells, in vivo imaging

INTRODUCTION

Oral route of drug administration provides greater extent of patient compliance as being one of the most convenient and cost-effective route compared to the others such as parenteral [1]. Asenapine maleate (ASPM) is an antipsychotic drug used in the treatment of schizophrenia and bipolar I disorder. However, the oral bioavailability of ASPM is low (<2%) [2, 3] due to its extensive metabolism in the liver. It is currently available as a sublingual tablet in the market.

ASPM exists in two polymorphic forms, namely monoclinic (H) and orthorhombic (form L) forms [4]. Although form L shows lower solubility than Form H, the marketed sublingual tablet of ASPM contains form L polymorph because the micronized product of form H in a pure polymorphic form could not be reproducibly manufactured [5]. Since the sublingual tablet formulation contains mixture of polymorphs, it tends to display unpredictable undesirable properties. Moreover, other demerits of sublingual route are the inconvenience of holding the dose in the mouth, tongue numbness and drug loss if swallowed. Since antipsychotics need to be taken for a longer period, oral route is better for patient compliance compared to other routes of administration.

Many studies have been conducted to develop different formulations of ASPM, including sublingual film [6], thermo-responsive *in situ* nasal gel containing ASPM-hydroxyl propyl β-cyclodextrin inclusion complex [7], nanostructured lipid carriers of ASPM for intranasal delivery [8], solid lipid nanoparticles of ASPM for oral delivery [9, 10]. Additionally, three patents are also available on intranasal [11], transdermal [12] and injectable [13] formulations of asenapine. Studies reported so far on the formulation development for ASPM do not include the nanostructured lipid carriers (NLCs) for oral delivery. Moreover, the demerits of ASPM sublingual tablets suggest the need of a formulation of ASPM that can be administered with increased bioavailability. Thus, with the nanotechnology approach we endeavored to develop novel nanostructured lipid carriers of ASPM. The study was based on hypotheses that NLCs will get access into intestinal lymphatic system (ILS) after oral administration and will improve the bioavailability of ASPM. The mechanism behind lymphatic transport of NLCs is not yet completely understood. However, it has been suggested that the lipid formulations on oral administration stimulate the synthesis of chylomicrons by the enterocyte and the subsequent association of drug with the chylomicrons promotes drug uptake into ILS [14, 15]. ILS plays an important role in evading first pass metabolism as lymph vessels drain directly into systemic

circulation *via* thoracic duct thereby circumventing portal circulation [16, 17]. NLCs are new generation of solid lipid nanoparticles (SLNs), prepared with spatially different lipids such as solid and liquid lipids (oils) to obtain nanoparticles with imperfect crystal lattice. Due to such imperfections drug-loading capacity is enhanced and drug expulsion during storage is minimized [18].

In routine, formulation optimization process involves collection of data by changing one factor at a time (OFAT) while keeping other factors constant and analyzing it by aid of either graphical or statistical methods. This OFAT approach is time consuming and does not lay any knowledge on the effects of interaction between factors. In such cases, design of experiments (DoE) is a useful approach in formulation optimization. DoE is a statistical multivariate optimization method wherein simultaneous analysis of multiple factors at different levels can be carried out. This ensures detection of effects on outcome due to individual factors in addition to effects of interaction between factors in minimum experimental runs, thereby cutting down the time required for optimization [19]. Thus, we aimed to develop and optimize ASPM-NLCs by statistical experimental design approach using Design-Expert® software, 9.0.4.1 version (Stat-Ease, Inc. Minneapolis, MN). The independent variables having significant effect on dependent variables such as particle size, polydispersity index (PDI), zeta potential (ZP) and percentage entrapment efficiency (%EE) were screened by Plackett-Burman design and the selected significant factors were further optimized by Response surface methodology *i.e.* Box-Behnken design. The independent variables statistically optimized were total lipid amount (% w/v), surfactant concentration (% w/v), oil content (% wrt total lipid), lipid: drug ratio, sonication parameters such as amplitude (%), pulse (s) and time (min), and temperature (ºC). Key end points and techniques for the developed NLCs were particle size and charge (by Malvern ZetaSizer), surface morphology (by transmission electron microscopy), entrapment efficiency (by HPLC), In vivo organ biodistribution and quantification (by SPECT imaging and gamma counting, respectively), and in vivo preclinical pharmacokinetics and efficacy studies (in Wistar rats).

MATERIALS AND METHODS

Materials

ASPM was generously gifted by MSN Organics Pvt. Ltd. (Hyderabad, Telangana State, India) and Orbicular Pharma Tech Research and Development (Hyderabad, Telangana State, India). Letrozole, used as an internal standard in this study was obtained from Gland Pharma Pvt

Ltd., Malur, Karnataka State, India. Glyceryl monostearate (GMS) and glyceryl monolaurate (GML) were obtained from Fine organics (Mumbai, India) as a gift samples. Compritol 888 ATO, Precirol ATO 5, Gelucire 50/13 and Labrafil M2125CS were obtained as a gift samples from Gattefosse (St-Priest, Cedex, France). Dynasan 116, Dynasan 118 and Softisan 154 were obtained as gift samples from Cremer Oleo GmbH & Co. KG (Witten, Germany). Glyceryl monooleate (GMO) was gifted by Mohini organics Pvt. Ltd. (Mumbai, India). Soyabean and Peanut oil were procured from Rajesh Chemicals Co. (Mumbai, India). Corn oil, olive oil and cottonseed oils were procured form Genuine Chemical Co. (Mumbai, India). Oleic acid, Sephadex G-100, phosphate buffer saline (PBS), Lucifer yellow, Fluorescein isothiocyanate (FITC) and fetal bovine serum (FBS) were purchased from Sigma Aldrich (St Louis, MO, USA). Stearic acid and cetyl palmitate were gifted by Encube Ethicals Pvt. Ltd. (Goa, India). Tween 20 and Tween 80 were procured from Nice Chemicals Pvt. Ltd. (Mumbai, India). Cremophor RH 40, Cremophor EL, Poloxamer 188, Poloxamer 407 were generously gifted by BASF India Ltd. (Mumbai, India). Methanol (HPLC grade), tert-butyl methyl ether (TBME) and potassium dihydrogen phosphate were procured from SD Fine Chemicals Ltd. (Mumbai, India). Hanks' Balanced salt solution (HBSS), 4-(2-hydroxyethyl)-1-piperazineethanesulfonic acid (HEPES), Dulbecco's Modified Eagle's Medium (DMEM), antibiotic-antimycotic solution and Trifluoroacetic acid (TFA) were procured from Himedia Laboratories Pvt. Ltd. (Mumabi, India). Acetonitrile (HPLC grade) and Triethylamine (TEA) were obtained from Merck Ltd. (Mumbai, India). Disodium EDTA was procured from Labort Fine Chem Pvt. Ltd. (Mumbai, India). Indium-111 chloride was obtained from Mallinckrodt (Netherlands). 1,2-distearoyl-sn-glycero-3-phosphoethanolamine-N-diethylenetriaminepentaacetic acid (ammonium salt) (DSPE-DTPA) was purchased from Avanti Polar Lipids, Inc (USA). Thin layer chromatography (TLC) strips for radiolabelling were purchased from Agilent Technologies UK Ltd. (Wokingham, UK). NAP-5 desalting columns were obtained from GE Healthcare Life Sciences (UK). Ultrapure water obtained from a Millipore Direct-Q® 3 water purification system (Millipore Corporation, Billerica, MA, USA) was utilized in the formulation processing. Caco2 cells (Human epithelial colorectal adenocarcinoma cells) were obtained from National Centre for Cell Science (NCCS), Pune, India. All other chemicals used were of reagent or analytical grade unless otherwise specified.

Saturation solubility study of ASPM: Saturation solubility of ASPM was determined at different pH conditions. Detailed method is described in Supplementary Information (SI).

RP-HPLC analytical method for quantification of ASPM: ASPM was estimated by an RP-HPLC method. Detailed method is described in SI.

Drug-excipients compatibility study

Compatibility between ASPM and the excipients was accessed by Fourier Transform Infra-red (FTIR) spectroscopy and DSC. Plain drug, solid lipid, physical mixture of drug and solid mixture (1:1% w/w) and physical mixture of drug and all the excipients involved in NLCs were subjected to FTIR and DSC studies. In FTIR, potassium bromide pellet press technique was used and the obtained pellet was placed in Shimadzu FTIR 8300 Spectrophotometer (Shimadzu, Tokyo, Japan) which was screened in the wavenumber range of 400 to 4000 cm^{-1}. DSC-60 calorimeter (Shimadzu, Kyoto, Japan) was used in DSC analysis wherein samples were placed in an aluminum pan, sealed and heated under nitrogen flow (50 mL/min) at a scanning rate of 5 °C/min from 30 °C to 250 °C. The heat flow as a function of temperature was measured.

Screening of excipients

The excipients (solid lipid, oil and surfactant) involved in the preparation of NLCs were screened by conducting solubility study of ASPM in different solid lipids (Gelucire 50/13, Precirol ATO 5, Softisan 154, Dynasan 116, Dynasan 118, Campritol 888 ATO, Glyceryl monostearate, Cetyl palmitate and Stearic acid), oils (Olive oil, cotton oil, corn oil, peanut oil, soyabean oil, oleic acid, glyceryl monooleate, Labrafil M2125CS, Labrafac PG, Migloyl 810) and 1% w/v surfactant solution (Labrasol, Cremophor EL, Tween 80, Tween 20, Poloxamer 407 and Poloxamer 188). ASPM was added in increment to the solid lipid (1.0 g) which was melted at 5 °C above the melting point of lipid. Any undissolved drug in molten lipid was visually observed and after complete dissolution at saturation point, the lipid/drug mixtures were cooled down to room temperature for solidification. Calorimetric analysis was performed on the solid mixture using differential scanning calorimetry (DSC) to detect any presence of undissolved drug [20-22].

For screening oils and surfactants, known amount of drug in excess was added to 1.0 mL of oil (or surfactant solution) and samples were kept in a shaking water bath at 37 ± 2 °C for 48 h. After equilibrium, samples were centrifuged at 10000 rpm for 10 min. Supernatants were diluted appropriately with methanol, filtered and analyzed by RP-HPLC [23, 24].

Preparation of NLCs

ASPM-NLCs were prepared by ultrasound dispersion method as previously reported [25, 26]. GMS and oleic acid were chosen as solid lipid and oil, respectively, based on the solubility

study of ASPM in lipids. GMS and oleic acid mixtures were melted at 70 ºC and accurately weighed ASPM was added to the molten lipid. Tween 80 was chosen as the surfactant and its aqueous solution which was maintained at 70 ºC was added to the melted lipid mixture. The resultant coarse emulsion was sonicated (Probe sonicator VC 130, Sonics and Materials Inc, USA) for 10 min and cooled in ice bath for 15 min for lipid solidification and formation of NLCs.

Statistical optimization of NLCs

The independent variables in Plackett-Burman and Box-Behnken design are given in Table 1. The details of experimental batches of NLCs formulation in Plackett-Burman and Box-Behnken design are given in Table S1 and Table S2 (SI), respectively. Methodology involved in *Screening of independent variables (by* Plackett-Burman design) and *Optimization of independent variables by response surface methodology (*Box-Behnken response surface design) is detailed in SI (S3).

Characterization of NLCs

Particle size, PDI and zeta potential: The average particle size, PDI and ZP of the prepared NLCs were determined by Malvern Zetasizer (Nano ZS, Malvern Instruments, UK).

Particle concentration: The concentration of particles in the dispersion of NLCs was determined by Nanoparticle Tracking Analysis (NTA) (NanoSight, Malvern Instruments, UK). Samples were diluted appropriately to obtain 30 to 60 particles per image frame and measured in triplicate.

Entrapment efficiency: Gel chromatographic separation technique was used to purify ASPM-NLC dispersion from un-entrapped free drug using Sephadex G-100 column (2.5 cm length × 1.0 cm i.d.) [27-29]. Sephadex G-100 was soaked in distilled water (80 °C) overnight and was then loaded into 2.5 mL syringe. Before sample elution, column was centrifuged at 2,000 rpm for 2 min to obtain a dehydrated column. Later, the column was rehydrated with 0.5 mL of water and subsequently, 0.5 mL of nanoparticle dispersion was passed through the column followed by elution with 1 mL of water. The opalescent eluent containing NLCs was collected and ruptured using chloroform and methanol mixture (2:1% v/v). The resultant solution was diluted with RP-HPLC mobile phase and filtered through 0.22 μm membrane syringe filter before injecting into HPLC. Entrapment efficiency was calculated using the formula.

$$\text{Entrapment efficiency (\%)} = \frac{[ASPM]_E}{[ASPM]_T} \times 100$$

where, $[ASPM]_E$ represents the amount of encapsulated drug and $[ASPM]_T$ represents the total ASPM content in nanoformulation.

DSC, FTIR and X-Ray Diffraction (XRD) studies: To access any change in crystalline nature of drug when encapsulated in NLCs, plain drug and lyophilized optimized NLC formulation was subjected to XRD, FTIR and DSC studies. The XRD pattern was recorded using a Philips, PW-171 X-ray diffractometer with Cu-NF filtered CuKα radiation in the 2θ range of 0-80°. DSC and FTIR analyses were performed for the samples as per the procedure mentioned under "*Drug-excipients compatibility study" section.* For lyophilization, ASPM-NLCs dispersion was centrifuged at 22000 rpm for 45 min at 4 ºC. The separated supernatant was further centrifuged at same condition and the pellet obtained in both the steps was re-dispersed in 5% w/v sucrose cryoprotectant solution. The solution was frozen for 8 h at -80 ºC followed by drying at -48 ºC for 48 h using freeze dryer (LFD-5508, Daihan Labtech Co. Ltd., Korea). For the optimization of cryoprotectant and its concentration, various cryoprotectants such as mannitol, sucrose, maltose, dextrose, lactose and trehalose (at the concentrations of 5% w/v) were assessed with respect to change in particle size after lyophilization and the optimum cryoprotectant was used.

Transmission Electron Microscopy: Shape and surface morphology of optimized ASPM-NLCs were studied using transmission electron microscopy (TEM; CM200 Supertwin System, Philip, Netherlands). A drop of ASPM-NLCs sample was placed on a copper grid which was coated with carbon film and air dried for 1 min. Excess sample was drained off from the side with the help of filter paper. Sample was then quickly stained with phosphotungstic acid solution (1% w/v, pH 6.0) and air dried for 1 min followed by drying under IR lamp for 30 min. Sample loaded copper grid was then examined in TEM instrument at voltage 200 KV and resolution 0.23 nm.

In vitro drug release study*: In vitro* drug release studies of ASPM-NLCs were performed in 0.1 N HCl pH 1.2 for 2 h, ammonium acetate buffer pH 4.5 for 1 h, phosphate buffer pH 6.8 for 6 h and phosphate buffer pH 7.4 for 48 h by dialysis method. The sink condition was maintained throughout the in vitro drug release study [14, 30]. The NLCs dispersion (containing 2 mg of drug) was transferred into a dialysis bag (MWCO: 12,000 Da) and the bag was suspended individually in 100 mL of each medium. This set-up was kept on a magnetic stirrer with a speed of 100 rpm at 37 ± 0.5 ºC. Aliquots (2 mL) were withdrawn (at intervals of 0.25, 0.5, 0.75, 1 and 2 h for pH 1.2; 0.5 and 1 h for pH 4.5; 0.25, 0.5, 0.75, 1, 2, 4 and 6 h for pH 6.8 and 0.5, 1, 2, 4, 6, 8, 10, 12, 24, 36 and 48 h for pH 7.4) and replaced with same volume of fresh media. The

withdrawn sample was analyzed by RP-HPLC for the estimation of amount of drug released from ASPM-NLCs.

Cell studies

Caco2 cell monolayer model were used to demonstrate the cell viability, cell uptake and cell permeability with the ASPM solution and ASPM-NLCs.

Cell toxicity by MTT assay

In a 96-well plate, about 5000 cells/ well were grown in 100 µL of the supplemented DMEM medium+ 1% v/v penicillin–streptomycin for 24 h at 37 ºC in CO_2/ air atmosphere (5/95% v/v) for cell adhesion to occur. The cells were then treated with ASPM solution and ASPM-NLCs at different concentration ranges (1-20 µmol/mL) for 48 h at 37 °C. Medium was discarded and cells were rinsed with fresh culture media. Later, freshly prepared 3-(4,5-dimethylthiazol-2-yl)-2,5-diphenyltetrazolium bromide (MTT; 50 µL of 2 mg/mL solution prepared in PBS) was added to each well and plate was shaken gently and incubated for 3 h at 37 ºC in 5/95% v/v CO_2/air atmosphere. After 3 h, the supernatant was removed and the formazan crystals formed in the cells were solubilized by addition of 50 µL of iso-propanol. Absorbance was read in Microplate reader (ELx800, BioTek Instruments Inc., Winooski, VT, USA) at a wavelength of 540 nm.

Cell uptake study

Cells were seeded at a density of 5×10^5 cells per well in a Corning® Costar® 6-well flat bottom culture plate and incubated overnight at 37 ℃ in 5/95 (%v/v) CO_2/air atmosphere. After 24 h, it was replaced with fresh serum-free medium, and then the prepared FITC-labeled formulations were added to the cells at 2.57 µM concentration. After 2 h of incubation, the medium was discarded and the cells were washed three times with cold PBS. The cellular uptake profiles was determined by confocal laser scanning microscope (CLSM) (FV 1000 SPD, Olympus, USA).

Cell permeability study

Cells were seeded at a density of 10^5 cells/insert onto a Transwell® polycarbonate inserts (12 wells, 3 µm pore diameter). The culture medium (0.5 mL in the apical side and 1.5 mL in basolateral side) was replaced for 5 days following seeding and every 2 days thereafter. The quality of the monolayer was assessed by measuring TEER at 37 °C and determined by measuring the transport of Lucifer yellow across the cell monolayer at the end of each experiment. Only monolayers displaying TEER values above 400 Ω were used in the experiment. ASPM solution and ASPM-NLCs contained in 0.5 mL HBSS pH 7.4 was added on the apical side and 1.5 mL of

HBSS pH 7.4 on the basolateral side of the monolayer. After 4 h, ASPM concentration in the basolateral side was determined by RP-HPLC [31].

***Ex vivo* and *In vivo* studies**

Ex vivo and *in vivo* studies were carried out in male Sprague-Dawley rats, weighing 200-250g, which were bred at Central Animal Research Facility, Manipal Academy of Higher Education, Manipal. Prior to the study, approval from Institutional Animal Ethical Committee, Kasturba Medical College, Manipal, was obtained (Approval No: IAEC/KMC/42/2014) and animal handling was carried out as per the institutional and national guidelines for the care and use of animals. SPECT (Single photon emission computed tomography) and CT (Computed tomography) imaging was performed under the authority of project and personal licenses granted by the UK Home Office and the UKCCCR Guidelines (1998). Male Sprague-Dawley rats, weighing 200-250g, were purchased from Charles River (UK). Rats were housed in polypropylene cages at 25 ± 2 °C, exposed to light: dark cycle (12 h each), and had free access to food and water.

Everted rat ileum sac model

Ex vivo study to demonstrate the absorption of drug through ileum portion of small intestine was carried out by everted rat ileum sac model. Rats were fasted overnight before the day of the experiment. The rat were humanely sacrificed and small intestine was dissected out. The ileum portion (8 cm) was excised and flushed several times with Ringer's solution at pH 7.4 (NaCl (9 g/L), KCl (0.42 g/L), CaCl2 (0.24 g/L) and NaHCO3 (0.2 g/L)) to remove any chyme contents. The ileum was placed in a petri dish containing Ringer's solution. The solution was continuously bubbled with oxygen using aerator throughout the experiment. The ileum was pushed completely over a capillary tube (OD: 1.5 ± 0.05 mm), tied one end with thread and then gently everted the ileum. Perfusion apparatus was used which consisted of 'U' shaped glass tube (1 cm i.d., 25 mL capacity) with cannulated cut on one arm of the 'U' tube. The rat ileum was tied between cannulated parts of tube and then the apparatus was placed in a beaker containing 450 mL Ringer's solution. The ileum was completely dipped in Ringer's solution. The beaker containing solution was referred to as mucosal compartment, whereas the perfusion apparatus was referred to as serosal compartment. The whole apparatus was mounted on a magnetic stirrer and the experiment was carried out at 100 rpm and 37 °C. ASPM solution/ dispersion of ASPM-NLCs was added in the beaker and the sample was withdrawn from cannulated arm of the 'U' tube at time points between 1 and 3 h. The withdrawn volume was replaced with fresh Ringer's solution in the other

arm of the 'U' tube. The samples were analyzed by HPLC to measure the amount of drug absorbed from mucosal to serosal compartment.

Whole body SPECT/CT imaging of radiolabelled NLCs in rat

Radiolabelling of NLCs: Radiolabelled NLCs were prepared by the ultrasound dispersion method as described above with the incorporation of 1% w/w of total lipid of DSPE-DTPA in lipid phase (NLCs-DTPA) [32]. The ^{111}In solution (30 MBq) was added to 2 M ammonium acetate buffer (one ninth of the reaction volume, pH 5.5). This was then added to the NLCs-DTPA solution (73.7 mM of lipid) to give a final ammonium acetate concentration of 0.2 M. This mixture was incubated for 30 min at room temperature for reaction to occur. The reaction was quenched by the addition of 0.1 M EDTA solution to the mixture (5% v/v of the reaction mixture) to chelate free ^{111}In. The unbound [^{111}In]EDTA was removed by passing the radiolabeled NLCs though NAP-5 desalting column equilibrated with PBS. The sample was eluted through the column with 500 µL of PBS for each fractions and the eluent was collected in total 4 fractions (F1-F4).

Efficiency and stability of the radiolabelling in PBS and serum: The radiolabeled NLC fractions ([^{111}In]NLCs), F1 to F4 were spotted on glass microfiber thin layer chromatography (TLC) paper strips impregnated with silica gel. These TLC strips were then developed using a mobile phase of 0.1 M ammonium acetate pH 5.5 containing 25 mM EDTA. The developed strips were allowed to dry and counted quantitatively using a cyclone phosphor detector (Packard Biosciences, Perkin-Elmer Inc., UK). The radiolabelling stability was assessed by incubating the radiolabelled samples in PBS or FBS (1:1% v/v) for 24 h at 37 ºC. The percentage of ^{111}In remained conjugated to the NLCs was evaluated by TLC.

SPECT/CT imaging: Rats were orally administered with [^{111}In]NLCs containing 10.2 µmol lipid per 800 µL with radioactivity of 24 MBq using oral gavage. Rats were imaged with nano-SPECT/CT scanner (Bioscan ®, USA) 0–40 min, 4 h and 24 h post oral administration. A tomography was initially performed (45 Kvp; 1000 ms) to obtain parameters required for the SPECT and CT scanner, including the starting line, finish line and axis of rotation of the acquisition. SPECT scans were obtained using a 4-head scanner with 1.4 mm pinhole collimators and the following settings: number of projections: 24, time per projection: 60 s and duration of the scan 60 min. CT scans were obtained at the end of each SPECT acquisition using 45 Kvp. All data were reconstructed with MEDISO (Medical Imaging System) and the combining of the SPECT

and CT acquisitions were performed using InVivoScope^{TM} software (Bioscan, Washington DC, USA).

Pharmacokinetics study

For pharmacokinetic study in plasma, the rats were divided into 2 groups.

Group I: ASPM solution (p.o, n=6) and Group II: ASPM-NLCs (p.o, n=6). The plain drug solution and ASPM-NLCs dispersion was administered to rats using an oral gavage. Both groups received asenapine dose of 15.8 mg/kg rat body weight. Blood was withdrawn from retro-orbital sinus at the time points between 0.5 and 72 h in the tubes containing disodium EDTA. Blood was centrifuged at 5000 rpm for 10 min and the collected plasma after centrifugation was stored at -80 ºC until analysis. The amount of ASPM in plasma was analysed by RP-HPLC based bioanalytical method which is described in SI (S4) [33]. Pharmacokinetic parameters were calculated using Phoenix WinNonlin software version 6.4**.**

Tissue distribution study

Eighteen rats were allocated into two groups of 9 rats each for ASPM solution and ASPM-NLCs and they received the same dose of drug orally as described under "Pharmacokinetic study". In each group, the rats were subdivided into 3 groups (n=3), based on the time point of their sacrifice. At 1 h, 8 h, and 24 h post administration, the rats were sacrificed and brain, liver, kidney, spleen and small intestine were isolated. The collected organs were weighed and then homogenized with saline (1 mL to 3 mL) and 100 µL of TFA under ice-cold bath. The homogenates were centrifuged at 18000 rpm for 10 min at 10 °C in a cold centrifuge and the supernatant obtained was analyzed by RP-HPLC based bioanalytical method which is described in SI. The amount of drug distributed in organs at different time points was represented as concentration of drug per gram of tissue.

Pharmacodynamics studies

A psychostimulant induced hyperactivity model was used to study the pharmacodynamics of the formulated ASPM-NLCs. The model was developed by administering levodopa (L-dopa) and carbidopa to rats which causes increase in locomotor activity (LMA) [8]. Effect of formulation in reversing these conditions was studied. Rats were divided into four groups (n=4): Group I: Normal control group with no treatment, Group II: LMA induced rats (i.p. with L-dopa (10 mg/Kg) and carbidopa (2.5 mg/Kg)) with no treatment, Group III: LMA induced rats treated with ASPM solution (15.8 mg/Kg, p.o.), Group IV: LMA induced rats treated with ASPM-NLCs (15.8 mg/Kg,

p.o.). LMA was assessed for 5 min interval at 1 h, 2 h and 3 h by measuring locomotor count using Digital Photo Actometer (INCO, Ambala, India). The LMA in group II was assessed after 1 h of L-dopa-carbidopa administration. In group III and IV, ASPM was administered after 30 min of L-dopa-carbidopa administration and then LMA was noted after 30 min of ASPM administration.

Stability studies

Stability of ASPM-NLCs was assessed at storage condition of 5 ± 3 °C and 25 ± 2 °C/60 ± 5% RH as given in ICH guidelines Q1A R2 for 6 months. After 7, 15, 30, 60, 90 and 180 days, the stability charged samples (NLCs dispersion) were analyzed for particle size, PDI, zeta potential and entrapment efficiency.

Statistical analysis

GraphPad Prism 5.03 (Graph Pad Software Inc. CA, USA) was used for statistical analysis of data obtained. The data is represented as mean ± SD unless otherwise specified. Unpaired t-test at 5% significance level was used to obtain two-tailed *p* value for two group data and one-way ANOVA followed by Tukey's post-hoc test was utilized for multiple group comparison.

RESULTS

Solubility study

Saturation solubility was found to be 3.4 ± 0.2 mg/mL in water; 11.3 ± 0.5 mg/mL in pH 1.2 HCl buffer; 5.4 ± 0.3 mg/mL in pH 4.5 acetate buffer; 2.8 ± 0.2 mg/mL in pH 6.8 phosphate buffer; 2.6 ± 0.3 mg/mL in pH 7.4 phosphate buffer and 1.2 ± 0.5 mg/mL in pH 9.2 borate buffer. ASPM showed maximum solubility in GMS (Fig. 1A). This is supported by the DSC thermogram of solid mixture of ASPM and GMS (obtained during lipid screening study), in which the endothermic peak of the drug was negligible (Fig. 2C). ASPM showed negligible solubility in vegetable oils (Fig. 1B); but showed high solubility in oleic acid (Fig. 1C). ASPM did not show much difference with respect to solubility in the presence of various surfactants studied.

Drug-excipient compatibility studies

The FTIR spectrum of ASPM showed characteristic peaks at wavenumber 2960 cm^{-1}, 3037 cm^{-1}, 1614 cm^{-1}, 1572 cm^{-1}, 1483 cm^{-1} and 1047 cm^{-1} (Fig. S1A in SI). The comparison between FTIR spectrum of ASPM with GMS (Fig. S1B in SI), ASPM-GMS mixture (1:1) (Fig. S1C in SI) and physical mixture containing drug, solid lipid, oleic acid (oil), and sucrose (cryoprotectant) in weight ratio of 1:1:1:1 (Fig. S1D in SI**)** revealed no considerable changes in the drug peaks in the

presence of lipid, indicating the absence of any chemical incompatibility between drug and lipid. The comparison between FTIR spectrum of placebo (Fig. S1E, SI) and ASPM-NLCs formulation (Fig. S1F, SI) indicated the presence of specific functional groups of GMS and other excipients in ASPM-NLCs same as in placebo which demonstrated the absence of any interaction between ASPM and the excipients used.

In the DSC studies, plain drug showed an endothermic peak at 146.23 °C (Fig. 2A); whereas in the presence of GMS, ASPM melting endotherm was observed at 141.87 °C with GMS getting melted at 61.20 °C (Fig. 2B). The solid mixture of drug and GMS obtained during lipid screening study showed no endothermic peak for ASPM. However, there was little disturbance in the baseline at ASPM melting range (Fig. 2C), which could be due to the presence of minute residual undissolved drug at saturation point of solubility.. In DSC thermogram of ASPM-NLCs, drug endothermic peak was not visible; in fact GMS and sucrose melting point peaks were observed at 58.27 ºC and 184.68 °C, respectively (Fig. 2D). The endotherm of sucrose was observed at 190.52 ºC in DSC thermogram of sucrose (Fig. 2E).

XRD

The XRD pattern of ASPM showed two characteristic peaks; one at a 2-theta value of 9.4º and other most intense peak at 21.7º (Fig. S2A, SI). GMS showed characteristic peaks at 19.3º, 20.4º, 21.4º and 23.2° (Fig. S2B, SI). In ASPM-GMS physical mixture, intense peaks were observed at 19.3°, 20.3°, 21.7° and 23.3° (Fig. S2C, SI). With sucrose, characteristic XRD peaks were observed at 11.5°, 13.2°, 18.5°, 19.6° and 24.5° (Fig. S2D, SI). The XRD pattern of placebo showed the presence of characteristic peaks at 11.7°, 13.1°, 18.8°, 19.5°, 20.7°, 21.9° and 24.6° (Fig. S2E, SI). In the XRD pattern of formulation, characteristic peaks were observed at 11.5°, 12.9°, 18.6°, 19.3°, 21.8° and 24.5º (Fig. S2F, SI).

Statistical optimization of NLCs

In Plackett-Burman design, the independent variables were - i) total lipid amount (1-2% w/v), ii) surfactant concentration (1-2% w/v), iii) oil content (10-30% with respect to total lipid), iv) lipid/ drug ratio (10-30), v) sonication amplitude (40-80%), vi) sonication pulse (3-9 s), vii) temperature (70-90 ºC) and viii) sonication time (5-15 min). The dependent variables (responses) were i) particle size (nm), ii) PDI, iii) zeta potential (mV) and iv) % entrapment efficiency. Half-normal plots (Fig. S3: 1a, 2a, 3a and 4a; SI) and Pareto charts (Fig. S3: 1b, 2b, 3b and 4b; SI) were used for checking the significance of independent variables. ANOVA was carried out which

showed $p< 0.05$ for significant factors. Lipid amount and surfactant concentration were found to have significant effect on particle size, PDI and entrapment efficiency; whereas lipid/ drug ratio and surfactant concentration had significant effect on zeta potential. Overall, 3 out of 8 independent variables were found to influence either of the dependent variables. Although sonication amplitude did not show any significant impact on dependent factors in the software, 60% amplitude produced smaller sized particles than 40% and 80% in the actual experimental set-up. Moreover, at 80% amplitude, increase in particle size and turbidity of dispersion was observed.

The four factors *viz.* total lipid amount, surfactant concentration, oil content and lipid/drug ratio were optimized further by Box-Behnken response surface methodology design. As observed in contour plots (Fig. S4, SI), total lipid had a significant positive effect on particle size, PDI and entrapment efficiency, whereas surfactant concentration had a negative influence on the particle size, PDI and entrapment efficiency. Zeta potential was found to be low, ranging from +3.48 mV to -13 mV and only lipid/ drug ratio showed significant influence on zeta potential ($p< 0.05$). The increase in oil content did not appreciably increased entrapment efficiency.

The optimum solution consisting of 1.5% w/v total lipid, 2% w/v of surfactant concentration, 20% oil content and lipid/ drug ratio of 20 gave the desirability value of 1.000 and these optimized independent factors yielded data responses with values falling within 95% prediction interval (α=5%) and showed non-significant ($p> 0.05$) percent relative error (Table 2).

Freeze drying of NLCs

Among all the cryoprotectants tested, mannitol and sucrose showed particle size less than 500 nm and both resulted in free flowing powder at 5% w/v concentration (Fig. 3A). Sucrose was chosen as a suitable cryoprotectant for ASPM-NLCs freeze drying because it yielded comparatively lower particle sized lyophilized powder (252.10 ± 20.10 nm).

Transmission electron microscopy

TEM photomicrograph of optimized ASPM-NLCs formulation (Fig. 3B) showed spherical shaped particles which exhibited narrow size distribution (≈ 100 nm).

***In vitro* drug release study**

The *in vitro* release of ASPM from optimized NLC formulation was observed to be 22.3 ± 3.2% in pH 1.2 in 2h, 17.4 ± 1.6% in pH 4.5 in 1 h, 48.1 ± 2.8% in pH 6.8 in 6 h and 88.3 ± 3.1% in pH 7.4 in 48 h (Fig. 3C and 3D)

Cell line studies

FITC labelled NLCs showed significantly higher uptake in Caco2 cell lines compared to free dye (Fig. S5, SI). Although NLCs showed high uptake into cells, viability of cells treated with ASPM-NLCs was similar to plain drug treated cells. Plain drug and ASPM-NLCs were found to be non-cytotoxic as more than 80% cells were viable even at maximum ASPM concentration of 20 µM/mL (Fig. 4A). ASPM-NLCs showed significantly greater ($p< 0.001$) apparent permeability (*P*app) compared to plain drug ($24.2 \pm 1.5 \times 10^{-6}$ *vs.* $4.1 \pm 0.3 \times 10^{-6}$ cm/sec) (Fig. 4B).

Everted rat ileum sac technique

NLCs loaded with ASPM showed significant ($p< 0.01$) increase in *P*app value compared to plain drug at 1 h and 2 h. However at 3 h, the *P*app value of plain drug ($21.40 \pm 4.03 \times 10^{-5}$ cm/sec) was almost near to *P*app value of NLCs ($25.42 \pm 3.35 \times 10^{-5}$ cm/sec) (Fig. 4C).

Whole body SPECT/CT imaging of radiolabelled NLCs in rat

NLCs-DTPA containing 1% w/w of total lipid of DSPE-DTPA was radiolabelled with ^{111}In and the radiolabelling efficiency was found to be 73.4%. Stability of the radiolabelled NLCs was carried out at 37 °C in both PBS and 50 % FBS for 24 h in order to mimic the stability of these samples in *in vitro* and *in vivo* conditions, respectively. [^{111}In]NLCs were completely stable in PBS after 24 h incubation, whereas slightly reduced stability was observed in the presence of serum in which 92.2% and 96.8% of the ^{111}In remained bound to the NLCs for fractions F1 and F2, respectively. Radiolabelling efficiency of NLCs with Indium (^{111}In) is shown in Fig. 5A. TLC of purified radiolabelled NLCs after incubation with phosphate buffer saline (PBS) and fetal bovine serum (FBS) is shown in Fig. 5B.

Dynamic biodistribution of NLCs was assessed by whole body SPECT/CT imaging after oral administration. As shown in Fig. 5C, [^{111}In]NLCs entered stomach and some quantity reached small intestine during the first 40 min following oral gavage. At 4 h post administration, some amount of [^{111}In]NLCs remained in stomach and more entered small intestine and cecum. At 24 h, most of the [^{111}In]NLCs were excreted with low signals detected in the GI tract.

Pharmacodynamics study

The control animals (no treatment) showed normal locomotor activity (LMA) in digital Actophotometer (Locomotor counts: 1 h: 278 ± 57; 2 h: 385 ± 28; 3 h: 344 ± 39). The basal LMA in untreated rats (control) were recorded for comparison with other groups. The i. p. administration of L-Dopa and carbidopa at a dose of 10 mg/kg and 2.5 mg/kg, respectively in positive control rat

group showed a significantly ($p< 0.001$) increased LMA with maximum locomotor counts (1 h: 512 ± 38; 2 h: 615 ± 32; 3 h: 690 ± 40) compared to basal LMA (Fig. 6A). The plain drug at the asenapine equivalent dose of 15.8 mg/Kg showed a significant ($p< 0.001$) reduction in locomotor count (1 h: 142 ± 62; 2 h: 144 ± 30; 3 h: 102 ± 23) compared to positive control and normal control which was further reduced with ASPM-NLCs (1 h: 58 ± 8; 2 h: 42 ± 8; 3 h: 31 ± 11) (Fig. 6A).

Pharmacokinetics study

The mean plasma concentration-time profile of plain drug and ASPM-NLCs in rats following oral administration at asenapine equivalent dose of 15.8 mg/kg is shown in Fig. 5B and the corresponding pharmacokinetics parameters are summarized in Table 3. Marketed sublingual tablet of ASPM possess a terminal half-life ($t_{1/2}$) value of ≈ 24 h [3] ; whereas the $t_{1/2}$ value was found to be 31.6 ± 2.1 h in plain drug and 54.3 ± 0.6 h in NLCs after oral administration in rats. The elimination rate constant was low in both plain drug (0.0220 ± 0.0015 h^{-1}) and ASPM-NLCs (0.0128 ± 0.0002 h^{-1}). Also, ASPM showed high volume of distribution (V_d) and is retained longer in the body with mean residential time of 26.2 ± 0.7 h in plain drug and 22.7 ± 0.2 h in ASPM-NLCs. Plain drug showed high clearance of 403.74 ± 14.70 mL/h in rat, whereas ASPM-NLCs showed remarkably low clearance of 275.14 ± 19.61 mL/h ($p< 0.01$) compared to that of plain drug. ASPM-NLCs showed significant increase in AUC_{0-t} compared to plain drug (10101.74 ± 683.23 *vs.* 7309.06 ± 458.23 h*ng/mL, $p< 0.001$). The time to achieve maximum concentration of drug in plasma was much higher in ASPM-NLCs (8 h) than in plain drug (1 h). In case of ASPM-NLCs, two peaks were observed in the pharmacokinetic profile at 1 h and 8 h; however, maximum concentration (Cmax) of 420.43 ± 14.50 ng/mL was observed at 8 h.

Tissue distribution study

In tissue distribution study, plain ASPM showed significantly ($p<0.05$) higher concentration in small intestine at 1 h compared to liver, kidneys, spleen, brain and plasma (Fig. 6C). Highest accumulation of ASPM was found in spleen at 8 h, although there was high variation among rats (Fig. 6D). In 1 h, kidneys, liver and spleen showed almost similar value of drug accumulation but showed greater (≈3 times) tissue/ plasma ratio. The brain to plasma ratio of ASPM was 0.35 ± 0.22 at 1 h, 0.33 ± 0.13 at 8 h and 0.06 ± 0.02 at 24 h. Thus, ASPM concentration in brain was greater up to 8 h which then was declined by 24 h (Fig. 6E). Compared to plain ASPM, ASPM-NLCs showed high concentration of drug in the brain at all three time points. ASPM-NLCs showed more concentration of drug in spleen (1 h: 993.59 ± 108.86 ng/g; 8 h: 1111.98 ± 184.17

ng/g; 24 h: 416.14 ± 60.20 ng/g) in comparison to plain ASPM (1h: 618.83 ± 193.76 ng/g; 8 h: 795.52 ± 292.18 ng/g; 24 h: 72.63 ± 3.35 ng/g).

Stability study

Total drug content of the optimized formulation (prepared with 7.5 mg of drug in 10 mL of formulation) was found to be 7.31 ± 0.45 mg/10 mL of dispersion (≈ 97.5%). ASPM-NLCs were found to be stable at 5 ± 3 °C up to a period of 3 months with respect to size (within ≈100 nm), PDI (≈0.3) and drug content (>90%). However, at 25±2°C/60±5% RH, the ASPM-NLCs were stable up to 30 days with respect to size and PDI; but drug content was found to be <90% after 15 days.

DISCUSSION

Solubility study

ASPM being a basic drug has more affinity towards acidic pH as explained by Henderson-Hasselbalch equation resulting in high solubility in pH 1.2 [34]. The solid lipid and oil which has great potential for dissolving drug were preferred for preparation of NLCs as they will avoid partitioning of drug from lipid nanoparticles to surrounding aqueous media upon storage. The oil incorporated into NLCs helps in crystallizing the solid lipid in imperfect crystalline lattice which increases drug loading and decreases drug expulsion during storage [35]. Vegetable oils were preferred as they are unmodified dietary oils but ASPM showed negligible solubility in vegetable oils and hence, synthetic oils were screened further by solubility study [14]. Surfactant with least drug solubility was selected as it aids in retaining the drug in the lipid core and imparts firm association of drug with the lipid matrix [14]. Tween 80 was selected as it is known to enhance the drug delivery to brain [36]. Tween 80 coating over nanoparticles leads to adsorption of ApoE from plasma upon nanoparticle surface and this interacts with LDL receptors in BBB thereby accessing into brain by endocytic uptake mechanism. Also, non-ionic surfactants such as Tween 80 were preferred over ionic surfactants for oral preparations as they exhibit less toxic and irritation effect [37]. In addition, Tween 80 effectively inhibits the *in vivo* degradation of lipid matrix as the poly(ethylene oxide) (PEO) chains on the non-ionic surfactants hinder the anchoring of the lipase/co-lipase complex on lipid matrix that is responsible for lipid degradation [38].

Drug-excipient compatibility study

The characteristic peaks observed in the FTIR spectrum of ASPM correspond to sp3 C-H stretch (2960 cm^{-1}), sp2 C-H stretch (3037 cm^{-1}), aryl C=C (1614 cm^{-1}), =C-H functional group of aryl ring (1572 cm^{-1} and 1483 cm^{-1}) and –C-O bond (1047 cm^{-1}). FTIR spectroscopy demonstrated the absence of any interaction between ASPM and the excipients used as the comparison between FTIR spectrum of ASPM, GMS and ASPM-GMS mixture (1:1) revealed no considerable changes in the drug peaks in the mixture. Also, ASPM-NLCs and placebo NLCs spectra were similar showing the presence of excipient peaks in ASPM-NLCs same as in placebo.

The sharp endothermic peak of ASPM melting point at 146.23 ºC suggested the crystalline nature of drug. The drug endothermic peak was very small and less intense in DSC thermogram of ASPM-GMS physical mixture indicating that the drug was getting solubilized in molten GMS before reaching its melting temperature [39]. The slight decrease in melting point of ASPM compared to plain drug thermogram may be due to moistening effect of melted GMS [40]. The ASPM content in ASPM-GMS physical mixture is reduced to half compared to plain drug. So accordingly the heat required to melt the physical mixture could have been half of that required for plain drug. The heat of melt in plain drug is -63.03 J/g and in physical mixture is -5.84 J/g. Also, the onset of ASPM endothermic peak is less in physical mixture compared to plain drug ((141.87 °C and 146.23 °C for physical mixture and plain drug, respectively). This might indicate that the drug got moistened by molten GMS before reaching its melting temperature. Calorimetric analysis of solid mixture of drug and GMS obtained during lipid screening study supported the fact that drug got solubilized completely in GMS during the screening study as drug endothermic peak was negligible. There was little baseline disturbance at ASPM melting range which might be due to the presence of minute residual undissolved drug at saturation point of solubility. Absence of ASPM endotherm in formulation indicated the loss of crystallinity of drug by being molecularly dispersed in lipid matrix [14]. The different melting temperature of sucrose in formulation and plain sucrose may be because of the fact that sugar crystals possess varying melting properties, which result in melting temperature range (160–190 ºC), instead of a specific melting point; accordingly different melting points for sucrose are also observed in previous literature [41].

XRD

XRD pattern of placebo showed the presence of characteristic peaks corresponding to sucrose at 11.7°, 13.1°, 18.8° and 24.6°. The peak at 19.5° may be due to GMS or sucrose and at

20.7° and 21.9° corresponds to GMS. In XRD pattern of ASPM-NLCs, the peak at 21.8° may be because of GMS (and not due to ASPM), as the same peak at 21.9° was observed in placebo also. This would indicate the amorphization/ partial amorphization of ASPM in NLCs. In that case, the ASPM peak at about 9.4° cannot be interference in ASPM-NLCs; and no obvious peak was shown at about 9.4°. Similarly with DSC studies, the physical mixture of placebo NLC and ASPM would give more clarity by eliminating interference of low ratios of ASPM.

Statistical optimization of NLCs

In Pareto charts (Fig. S3, SI) obtained in Plackett-Burman design, terms above the Bonferroni limit are almost certainly significant; whereas those above the *t*-value limit are possibly significant and terms below the *t*-value limit are not likely to be significant. During sonication, 40% amplitude might be insufficient to decrease the particle size of ASPM-NLCs appreciably. However, 80% amplitude results in decrease in stability of dispersion which may be due to an increase in cavitation energy, leading to agglomeration [42]. Hence, amplitude of 60% was used in further optimization of ASPM-NLCs.

From contour plots (Fig. S4, SI), it was observed that size was significantly ($p<0.05$) increased with total lipid. Because, at higher concentrations, lipids merge together and increase the viscosity of the lipid phase (inner phase), which could affect the shearing capacity of sonicator [43]. This may also be a reason for significant increase in PDI on increasing the total lipid amount. Entrapment efficiency was increased significantly ($p< 0.05$) with an increase in total lipid content. The increase in entrapment efficiency may be due to accessibility of more number mono-, di-, and triglycerides of lipid for solubilizing ASPM which offer more spare space to accommodate excessive drug. Also, increased viscosity of the lipid phase upon increasing the amount of lipid resulted in quicker solidification of the lipids thereby preventing drug diffusion into the aqueous phase [44]. Significant difference was not observed on zeta potential on increasing the amount of total lipid.

As the concentration of surfactant was increased, the size of the ASPM-NLCs was reduced. This indicates that surfactant concentration has a negative influence on the particle size. This could be because the droplets formed during the sonication are better stabilized upon increasing the concentration of surfactants. At higher concentration, more surfactant is available to cover the high surface area of smaller particles, thereby preventing the coalescence of the particles into bigger droplets. Furthermore, the presence of surfactants on the particle surface reduces the surface

tension between lipid and aqueous phase, facilitating the solid particle formation during the cooling phase of ASPM-NLCs preparation [43, 44]. Surfactant concentration had a negative influence on entrapment efficiency because maximum drug gets partitioned in surfactant layer upon increasing surfactant concentration, thereby reducing the amount of drug in lipid matrix. PDI was found to reduce with an increase in surfactant concentration. This could be because of better mixing effect due to reduction in interfacial tension between lipid and aqueous phase at optimum concentration of surfactant. Zeta potential was found to be low (+3.4 mV to -13 mV), which could be due to the coverage of ASPM-NLCs with Tween-80. Also, coverage of ASPM-NLCs by Tween-80 could also decrease the mobility of particle leading to lower zeta potential values [43]. However, Tween-80 offers steric stabilization to the ASPM-NLCs despite the low zeta potential [45].

Lipid/ drug ratio significantly affected only zeta potential. As the lipid/ drug ratio was increased, amount of drug was decreased, which resulted in shifting the zeta potential more towards negative side. When lipid/ drug ratio decreased, drug amount increased resulting in zeta potential values towards positive side [22].

The increase in oil content was found to reduce drug entrapment efficiency, however not significantly, which may be due to low solubility of ASPM in oleic acid compared to in GMS.

Freeze drying of NLCs

In this study, lyophilization of ASPM-NLCs was a troublesome process as high particle size was obtained with most of the cryoprotectants studied. This could be due to change in the properties of surfactant layer by removal of water during freeze drying and this increases the particulate concentration leading to particle aggregation [46]. Increase in particle size of lipid nanoparticles after freeze drying was also observed by Cavalli et al., 1997 [47].

***In vitro* drug release study**

Different pH conditions were used in *in vitro* drug release study to indicate the drug release from NLCs at different parts of the body after oral administration i.e. stomach (pH 1.2, 2h), duodenum (pH 4.5, 1h), small intestine (pH 6.8, 6h) and intestine as well as systemic environment (pH 7.4, 48h). We fixed the maximum time up to 48 h in pH 7.4 just to observe how much time was required for at least 80% of drug to release. The *in vitro* release of ASPM from NLC formulation was observed to be 22.30 ± 3.2% in pH 1.2 in 2 h. It has been reported that Tamoxifen-NLCs prepared with GMS and Labrafil WL 2609 BS showed cumulative drug release of 5.00 ±

3.21% in pH 1.2 in 2 h and 12.35 ± 4.03% in pH 6.8 in 6 h [14]. Compared to the mentioned literature, a comparatively high release in pH 1.2 and pH 6.8 in our current study may be due to partial degradation of lipid carrier. This suggests the need for protection of NLCs from gastric acidic content. However, considering the complexity involved in enteric coating procedure for nano-carriers, uncoated NLCs are generally used for oral delivery of drugs as reported previously [48-50], even though the resistance offered by NLCs in gastric pH is low to moderate level. In pH 7.4 phosphate buffer, ASPM-NLCs showed sustained release of 88.30 ± 3.1% in 48 h.

Cell studies

To demonstrate the interaction of ASPM-NLCs with intestinal epithelial cells *in vivo*, the ability of *in vitro* cell culture system to internalize the particles was assessed. FITC-NLCs showed significantly high uptake in Caco2 cell lines compared to free dye due to nano-size and endocytosis uptake pathway. It has been reported that particles with a size below 200 nm could effectively diffuse through the mucus and get internalize into epithelial cells by endocytosis mechanism. ASPM, ASPM-NLCs or any of the components of NLCs do not possess any adverse effects to the cells *in vitro*. Lipid based carriers such as NLCs deliver the drugs at the site of absorption in a dissolved form thereby improving their permeability much greater than plain drug solution [51]. The high permeability of nanocarriers may also be due to the presence of Tween 80 on the surface of carriers which causes increase in cell membrane permeability [52].

***Ex vivo* and *in vivo* studies**

ASPM-NLCs showed high permeation across rat ileum compared to plain drug and this could be due to increase in contact surface area of NLCs to the intestinal epithelial cell because of nano size. The lipidic nature of NLCs and Tween 80 coating over the surface of NLCs may be other reasons for increased membrane permeability. SPECT/CT system allows the visualization of biodistribution of NLCs in a real time manner with great sensitivity by tracking the ^{111}In bound to DSPE-DTPA. [^{111}In]NLCs were detected only in stomach and intestine. However, the release of ASPM from NLCs and the subsequent absorption and distribution of ASPM to other tissues would not be detected by SPECT/CT. In pharmacokinetics study, high $t_{1/2}$ value of ASPM suggests the slow elimination of drug which is also indicated by low elimination rate constant. Plain drug showed high clearance of 403.74 ± 14.70 mL/h in rat which implies that hepatic clearance is influenced primarily by changes in liver blood flow rather than by changes in the intrinsic clearance, i.e. the metabolizing enzymatic activity [53]. Compared to plain drug, ASPM-NLCs

showed significant increase in AUC_{0-t} compared to plain drug which may be due to its nano size and the avoidance of first pass metabolism by getting absorbed through lymphatic transport pathway. In case of ASPM-NLCs, the first peak at 1 h could be due to the amount of un-entrapped free drug which has released from ASPM-NLCs in 1 h. This may also be due to quick absorption of the drug immediately after administration. Thereafter, the drug from NLCs was released slowly thereby attaining maximum concentration by 8 h.

Although, the mechanism involved in uptake of NLCs into ILS is not yet clearly established, it is hypothesized that NLCs, like dietary fat, are surface degraded by enzymes to monoglycerides in the intestine. These monoglycerides form drug loaded micelles which are taken up by intestinal cell. In the intestinal epithelial cell, monoglycerides in association with fatty acids and phospholipids form chylomicrons. The drug gets associated with the chylomicrons and these chylomicrons due to large particle nature enter into lacteals rather than blood capillaries. The enzymatic degradation is a surface degradation, therefore the size of the drug loaded oil droplets decreases and when size is below 100 nm, they are taken up by lymphatic system, as explained in the previous reports [54-56]. The prolonged plasma level of ASPM could be due to small size of ASPM-NLCs droplets. It is reported that small sized NLCs are mucoadhesive and remain longer in the absorption window in the upper gut thereby showing prolonged plasma level [56].

The possible explanations for two peaks in the pharmacokinetic profile could be: i) enterohepatic recycling (a part of the amount previously absorbed is drained in intestine for reabsorption) [57], ii) gastric mobility variation [58] and/or iii) initial peak is due to quick absorption of NLCs from intestine and then nanoparticles are taken by phagocytic cells of the reticuloendothelial system (RES) in plasma. Due to high lipophilicity, drug diffuses across phagocytic cell membrane into the plasma giving the second peak at a later time [59]. The significant reduction in induced locomotor count in case of ASPM-NLCs indicates greater pharmacodynamics efficacy of NLCs loaded with ASPM in comparison with plain drug.

After oral administration, drug from the small intestine usually permeates through the intestinal epithelium and distributes into various organs tested via systemic circulation. Therefore, at initial time point of 1 h, highest drug concentration was observed in small intestine from which drug has to be absorbed through intestine into systemic circulation. As the time progressed, the drug concentration declined in small intestine. ASPM rapidly distributes after absorption in the body. Accordingly, it has been reported that ASPM possesses large volume of distribution,

indicating extensive extravascular distribution [3]. Distribution of drug from systemic circulation depends upon the differences in blood perfusion, tissue binding, regional pH and cell membrane permeability [60]. Most of the drugs are highly distributed to rich blood-supply tissues such as kidneys, liver and spleen due to blood perfusion rate of tissue [61]. The greater tissue/ plasma ratio of ASPM in case of kidneys, liver and spleen implied that the distribution of ASPM depends on the blood flow or perfusion rate of the organ. The brain is also well perfused but the drug distribution rate into the brain is determined primarily by permeability. Moreover, the penetration rate into the brain is slow for highly protein-bound drugs such as ASPM, which is reported to be 95% plasma protein bound drug including albumin and alpha1-acid glycoprotein [53, 60]. Thus in case of plain drug, drug concentration in brain was greater up to 8 h which then was declined by 24 h. Compared to plain ASPM, ASPM-NLCs showed high concentration of drug in the brain at all three time points. This indicates that more drug was available from ASPM-NLCs in the systemic circulation for ready access to brain. Moreover, Tween 80 coating over ASPM-NLCs surface may be other reason for high ASPM concentration in brain. Tween 80 coating over nanoparticles is known to enhance the drug delivery to brain by leading to adsorption of ApoE from plasma upon nanoparticle surface and this interacts with LDL receptors in BBB thereby accessing into brain by endocytic uptake mechanism [36, 62]. ASPM-NLCs showed more concentration of drug in spleen in comparison to plain ASPM. This may be because NLCs are taken up through intestinal lymphatic pathway into systemic circulation. However, some amount present in lymphatics gets accumulated into lymph organs such as spleen.

CONCLUSION

In the present study, ASPM-NLCs were prepared for bioavailability enhancement via lymphatic uptake. NLCs were developed using statistical experimental design (DoE) approach. DSC and XRD studies indicated the amorphized nature of ASPM in lipid matrix. NLCs showed greater apparent permeability across Caco2 cell lines and everted rat ileum. Confocal laser scanning microscopy images revealed high cell uptake of ASPM-NLCs. Bioavailability was greatly enhanced with ASPM-NLCs and L-DOPA-carbidopa induced locomotor count was reduced significantly compared to plain drug. High concentration of drug in spleen indicated the lymphatic transport pathway of NLCs. Thus NLCs were successfully developed which showed enhanced performance both *in vitro* and *in vivo*.

FUTURE PERSPECTIVE

In the current study, ASPM-NLCs showed possible targetability to ILS as suggested by high permeability in cell line and in everted rat ileum sac study and from the preclinical SPECT-CT images. However, further confirmation of precise targetability to ILS can be achieved by establishing the pharmacokinetic determination of drug in intestinal lymph vessel using validated lymphatic transport models. Detailed pharmacokinetic and pharmacodynamics behavior of ASPM-NLCs in comparison with marketed sublingual tablets and intravenous injection of ASPM and ASPM-NLCs can be studied to establish absolute and relative bioavailability of ASPM-NLCs.

SUMMARY POINTS

- Asenapine Maleate (ASPM) is an antipsychotic drug which undergoes extensive first pass metabolism thereby making the oral route inconvenient by conventional formulations. Therefore, the current study aims to prepare nanostructured lipid carriers (NLCs) of ASPM for intestinal lymphatic uptake to increase its oral bioavailability.
- NLCs loaded with ASPM (ASPM-NLCs) were prepared by ultrasound dispersion technique using glyceryl monostearate, oleic acid and Tween 80.
- Statistical experimental design (DoE) approach using Design-Expert® software was used for screening and optimization of various independent variables.
- FTIR and DSC studies indicated no incompatibility between drug and the excipients used and DSC and XRD studies further indicated the amorphized nature of ASPM in lipid matrix.
- The optimized formulation exhibited good physicochemical parameters, i.e. particle size of 84.91±2.14 nm, polydispersity index of 0.222±0.026, zeta potential of -4.83±0.29 mV and encapsulation efficiency of 86.9±1.8%.
- ASPM-NLCs showed greater permeability across Caco2 cell lines and everted rat ileum compared to plain drug.
- Confocal Laser Scanning Microscopy images clearly demonstrated high cellular uptake of ASPM-NLCs in Caco2 cells compared to plain drug.
- ASPM-NLCs showed greater preclinical oral bioavailability and higher efficacy in reducing the L-DOPA-carbidopa induced locomotor count compared to plain drug.

- Tissue distribution study of ASPM-NLCs showed high concentration of drug in brain and spleen.

FINANCIAL AND COMPETING INTERESTS DISCLOSURE

The authors gratefully acknowledge the Science and Engineering Research Board (SERB), Department of Science and Technology, Govt. of India, New Delhi for the financial assistance and funding. K. Al-Jamal acknowledges funding from Worldwide Cancer Research (12−1054). F. N. Faruqu is funded by the Malaysian government agency Majlis Amanah Rakyat (MARA).

ACKNOWLEDGMENTS

Authors are grateful to Manipal Academy of Higher Education, Manipal, India for providing necessary facilities. The authors are also thankful to MSN Organic Ltd. (Hyderabad, India), Orbicular Pharmaceutical Technologies Ltd. (Hyderabad, India), Gattefosse (St-Priest, Cedex, France), Cremer Oleo GmbH & Co. (KG, Werk Witten), BASF India Ltd (Mumbai, India), Mohini organics Pvt. Ltd. (Mumbai, India) and Fine organics (Mumbai, India) for providing gift samples of few of the materials used in the study.

REFERENCES

Papers of special note have been highlighted as: '*' – of interest, or "**" – of considerable interest.

1. Mutalik S, Manoj K, Reddy MS, Kushtagi P, Usha AN, Anju P, Ranjith AK, Udupa N.Chitosan and enteric polymer based once daily sustained release tablets of aceclofenac: in vitro and in vivo studies. *AAPS PharmSciTech.* 9(2): 651-659 (2008).
2. Center for Drug Evaluation and Research (2009): Saphiris (asenapine) sublingual tablets, Chemistry Review(s)-Accessdata FDA; NDA 22-117. http://www.accessdata.fda.gov/drugsatfda_docs/nda/2009/022117s000_ChemR.pdf. (Accessed on December 25, 2013).

   * **This document gives the chemistry review of Asenapine drug.**
3. Therapeutic Goods Administration (2011), Australian Public Assessment Report for Asenapine: AusPAR Saphris Asenapine Schering-Plough Pty Limited PM-2009-03233-3-1. http://www.tga.gov.au/pdf/auspar/auspar-saphris.pdf. (Accessed on December 25, 2013).

   * **This document gives the overview information of Asenapine product submitted to Therapeutic Goods Administration.**
4. Ventimiglia G, Barreca G, Magrone D, Polymorphic forms of asenapine maleate and processes for their preparation European patent EP 2 468 750 A1 (2012).
5. Heeres GJ, Crystal form of asenapine maleate. United States patent US 20080200671 (2008).
6. Kapadia YD, Sodha HP, Patel VP. Formulation development and evaluation of sublingual film of asenapine maleate. *Pharm. Sci. Monit.* 4(3), 190-209 (2013).
7. Kulkarni JA, Avachat AM. Pharmacodynamic and pharmacokinetic investigation of cyclodextrin-mediated asenapine maleate in situ nasal gel for improved bioavailability. *Drug. Dev. Ind. Pharm.* 43(2), 234-245 (2017).
8. Singh SK, Dadhania P, Vuddanda PR, Jain A, Velaga S, Singh S. Intranasal delivery of asenapine loaded nanostructured lipid carriers: formulation, characterization, pharmacokinetic and behavioural assessment. *RSC. Adv*. 6(3), 2032-2045 (2016).
9. Naik B, Gandhi J, Shah P, Naik H, Sarolia J. Asenapine maleate loaded solid lipid nanoparticles for oral delivery. *Int. Res. J. Pharm.* 8(11), 45-53 (2017).

10. Gambhire VM, Ranpise NS. Enhanced oral delivery of asenapine maleate from solid lipid nanoparticles: pharmacokinetic and brain distribution evaluation. *Asian J. Pharm.* 12(3), 152-161 (2018).
11. Van der Sterren JM, Van den Heuvel DM. Intranasal administration of asenapine and pharmaceutical compositions therefor. United State patent US 2008/0306133 A1 (2008).
12. Solomon WD, Transdermal compositions of asenapine for the treatment of psychiatric disorders. World patent WO 2010127674 A1 (2010)
13. Faassen WA, Kemperman GJ, Hendrikus Van LA. Injectable formulations containing asenapine and method of treatment using same. World patent WO 2010149727 A3 (2011).
14. Shete H, Patravale V. Long chain lipid based tamoxifen NLC. Part I: Preformulation studies, formulation development and physicochemical characterization. *Int. J. Pharm.* 454(1), 573-583 (2013).

    * **This article is good for preformulation studies of NLCs**.
15. Porter CJ, Charman WN. Intestinal lymphatic drug transport: an update. *Adv. Drug. Deliv. Rev.* 50(1), 61-80 (2001).

    ** **Good review paper for understanding digestion and absorption of lipids in the lymphatic transport.**
16. Managuli RS, Raut SY, Reddy MS, Mutalik S. Targeting the intestinal lymphatic system: a versatile path for enhanced oral bioavailability of drugs. *Expert Opin Drug Deliv.* 15(8), 787-804 (2018).
17. Khan AA, Mudassir J, Mohtar N, Darwis Y. Advanced drug delivery to the lymphatic system: lipid-based nanoformulations. *Int. J. Nanomedicine.* 8(1), 2733–2744 (2013).

    * **This paper provides a detailed review of novel lipid-based nanoformulations and their lymphatic delivery via different routes, as well as the in vivo and in vitro models used to study drug transport in the lymphatic system.**
18. Yoon G, Park JW, Yoon I-S. Solid lipid nanoparticles (SLNs) and nanostructured lipid carriers (NLCs): recent advances in drug delivery. *J. Pharm. Investig.* 43(5), 353–362 (2013).

    * **This review paper provides an overview of the preparation and characterization technologies for solid lipid nanoparticles and nanostructured lipid carriers.**

19. Curic A, Reul R, Moschwitzer J, Fricker G. Formulation optimization of itraconazole loaded PEGylated liposomes for parenteral administration by using design of experiments. *Int. J. Pharm.* 448(1), 189-197 (2013).
20. Dubey A, Prabhu P, Kamath JV. Nano structured lipid carriers: A novel topical drug delivery system. *Int. J. Pharm. Tech. Res.* 4(2), 705-714 (2012).
21. Prombutara P, Kulwatthanasal Y, Supaka N, Sramala I, Chareonpornwattana S. Production of nisin-loaded solid lipid nanoparticles for sustained antimicrobial activity. *Food. Control.* 24(1-2), 184-190 (2012).
22. Patel K, Padhye S, Nagarsenker M. Duloxetine HCl Lipid Nanoparticles: Preparation, Characterization, and Dosage Form Design. *AAPS PharmSciTech*, 13(1), 125-133 (2012).
23. Prajapati ST, Joshi HA, Patel CN. Preparation and characterization of self-microemulsifying drug delivery system of olmesartan medoxomil for bioavailability improvement. *J Pharm. (Cairo).* 2013, 1-9 (2013).
24. Managuli RS, Kumar L, Chonkar AD et al. Development and validation of a stability-indicating RP-HPLC method by a statistical optimization process for the quantification of asenapine maleate in lipidic nanoformulations. *J. Chromatogr. Sci.* 54(8), 1290-1300 (2016).

    * **This paper provides the RP-HPLC method details for asenapine quantification in lipid formulations and in solutions.**
25. Bose S, Michniak-Kohn B. Preparation and characterization of lipid based nanosystems for topical delivery of quercetin. *Eur. J. Pharm. Sci.* 48(3), 442-452 (2013).
26. Pathak P, Nagarsenker M. Formulation and evaluation of lidocaine lipid nanosystems for dermal delivery. *AAPS PharmSciTech.* 10(3), 985-992 (2009).
27. Zhang W, Li X, Ye T et al. Nanostructured lipid carrier surface modified with Eudragit RS 100 and its potential ophthalmic functions. *Int. J. Nanomedicine*. 9, 4305-4315 (2014).
28. Liu C-H, Chiu H-C, Wu W-C, Sahoo SL, Hsu C-Y. Novel lutein loaded lipid nanoparticles on porcine corneal distribution. *J. Ophthalmol.* 2014, 1-11 (2014).
29. Gu X, Zhang W, Liu J et al. Preparation and characterization of a lovastatin-loaded protein-free nanostructured lipid carrier resembling high-density lipoprotein and evaluation of its targeting to foam cells. *AAPS PharmSciTech.* 12(4), 1200-1208 (2011).

30. Li F, Weng Y, Wang L, He H, Yang J, Tang X. The efficacy and safety of bufadienolides-loaded nanostructured lipid carriers. *Int. J. Pharm.* 393(1-2), 203–211 (2010).
31. Derakhshandeh K, Hochhausa G, Dadashzadehc S. In-vitro cellular uptake and transport study of 9-Nitrocamptothecin PLGA nanoparticles across caco-2 cell monolayer model. Iran. *J. Pharm. Res.* 10(3), 425-434 (2011).
32. Hodgins NO, Al-Jamal WT, Wang JT et al. Investigating in vitro and in vivo alphavbeta6 integrin receptor-targeting liposomal alendronate for combinatory gammadelta T cell immunotherapy. *J. Control. Release.* 256, 141-152 (2017).
33. Managuli RS, Gourishetti K, Shenoy RR, Koteshwara KB, Reddy MS, Mutalik S. Preclinical pharmacokinetics and biodistribution studies of asenapine maleate using novel and sensitive RP-HPLC method. *Bioanalysis* 9(14), 1037-1047 (2017).
* **This paper provides the details on asenapine extraction method from biological matrices and quantification of asenapine in plasma and tissue matrices.**
34. Gutsche S, Krause M, Kranz H. Strategies to overcome pH dependent solubility of weakly basic drugs by using different types of alginates. *Drug. Dev. Ind. Pharm.* 34(12), 1277-1284 (2008).
35. Qiu L, Yang L, Zhou H et al. Encapsulation of oxaliplatin in nanostructured lipid carriers-preparation, physicochemical characterization and in vitro evalulation. *Asian J. Pharm. Sci.* 7(5), 352-358 (2012).
36. Das D, Lin S. Double-coated poly (butylcynanoacrylate) nanoparticulate delivery systems for brain targeting of dalargin via oral administration. *J. Pharm. Sci.* 94(6), 1343-1353 (2005).
37. Mcclements DJ, Rao J. Food-grade nanoemulsions: formulation, fabrication, properties, performance, biological fate, and potential toxicity. *Crit. Rev. Food Sci. Nutr.* 51(4), 285-330 (2011).
38. Shah R, Eldridge D, Palombo E, Harding I. Lipid Nanoparticles: Production, Characterization and Stability. Springer Briefs in Pharmaceutical Science & Drug Development (2015).
39. Samein LH. Preparation and evaluation of nystatin loaded-solid-lipid nanoparticles for topical delivery. *Int. J. Pharm. Pharm. Sci.* 6(2), 592-597 (2014).

40. Victoria MM, David CJ. Thermal and rheological study of lipophilic ethosuximide suppositories. *Eur. J. Pharm. Sci.* 19(2-3), 123-128 (2003).
41. Hurtta M, Pitkänen I, Knuutinen J. Melting behaviour of D-sucrose, D-glucose and D-fructose. *Carbohydr. Res.* 339(13), 2267-2273 (2004).
42. Sugita P, Ambarsari L, Farichah F. Increasing amount and entrapment efficiency of chitosan-ketoprofen nanoparticle using utrasonication method with varied time and amplitude. *IJRRAS.* 14(3), 612-618 (2013).
43. Martins S, Tho I, Souto E, Ferreira D, Brandl M. Multivariate design for the evaluation of lipid and surfactant composition effect for optimisation of lipid nanoparticles. *Eur. J. Pharm. Sci.* 45(5), 613-623 (2012).
44. Hao J, Fang X, Zhou Y et al. Development and optimization of solid lipid nanoparticle formulation for ophthalmic delivery of chloramphenicol using a Box-Behnken design. *Int. J. Nanomedicine* 6, 683-692 (2011).
45. Kasongo KW, Pardeike J, Muller RH, Walker RB. Selection and characterization of suitable lipid excipients for use in the manufacture of didanosine-loaded solid lipid nanoparticles and nanostructured lipid carriers. *J. Pharm. Sci.* 100(12), 5185-5196 (2011).
46. Mehnert W, Mader K. Solid lipid nanoparticles Production, characterization and applications. *Adv. Drug Deliv. Rev.* 47(2-3), 165-196 (2001).
47. Cavalli R, Caputo O, Carlotti ME, Trotta M, Scarnecchia C, Gasco MR. Sterilization and freeze-drying of drug-free and drug-loaded solid lipid nanoparticles. *Int. J. Pharm.* 148(1), 47-54 (1997).
48. Mishra A, Imam SS, Aqil M et al. Carvedilol nano lipid carriers: formulation, characterization and in-vivo evaluation. *Drug Deliv.* 23(4), 1486-1494 (2016).
49. Luan J, Zheng F, Yang X, Yu A, Zhai G. Nanostructured lipid carriers for oral delivery of baicalin: In vitro and in vivo evaluation. *Colloids Surf. A.* 466, 154-159 (2015).
50. Shah NV, Seth AK, Balaraman R, Aundhia CJ, Maheshwari RA, Parmar GR. Nanostructured lipid carriers for oral bioavailability enhancement of raloxifene: Design and in vivo study. *J. Adv. Res.* 7(3), 423-434 (2016).
51. Khan S, Baboota S, Ali J, Khan S, Narang RS, Narang JK. Nanostructured lipid carriers: An emerging platform for improving oral bioavailability of lipophilic drugs. *Int. J. Pharma. Investig.* 5(4), 182-191 (2015).

52. Staurouskaya AA, Potapova TV, Rosenblat VA, Serpinskaya AS. The effect of non-ionic detergent tween 80 on colcemid-resistant transformed mouse cells in vitro. *Int. J. Cancer.* 15(4), 665-672 (1975).
53. http://toxnet.nlm.nih.gov/cgi-in/sis/search/r?dbs+hsdb:@term+@rn+@rel+65576-45-6 (Accessed on 26 March 2017).
54. Olbrich C, Kayser O, Muller RH. Lipase degradation of Dynasan 114 and 116 solid lipid nanoparticles (SLN)--effect of surfactants, storage time and crystallinity. *Int. J. Pharm.* 237(1-2), 119-128 (2002).
55. Olbrich C, Muller RH. Enzymatic degradation of SLN-effect of surfactant and surfactant mixtures. *Int. J. Pharm.* 180(1), 31-39 (1999).
56. Muchow M, Maincent P, Müller RH, Keck CM. Testosterone undecanoate – increase of oral bioavailability by nanostructured lipid carriers (NLC). J Pharm. Technol. Drug. Res. 2(1), 1-4 (2013).
57. Plusquellec Y, Campistron G, Staveris S et al. A double-peak phenomenon in the pharmacokinetics of veralipride after oral administration: a double-site model for drug absorption. *J. Pharmacokinet. Biopharm.* 15(3), 225-239 (1987).
58. Wang Y, Roy A, Sun L, Lau CE. A double-peak phenomenon in the pharmacokinetics of alprazolam after oral administration. *Drug Metab. Dispos.* 27(8), 855-859 (1999).
59. Fang G, Tang B, Chao Y, Zhang Y, Xu H, Tang X. Improved oral bioavailability of docetaxel by nanostructured lipid carriers: in vitro characteristics, in vivo evaluation and intestinal transport studies. *RSC Adv.* 5(117), 96437-96447 (2015).
60. J. Le, Drug Distribution to Tissues (2016). Available online: http://www.msdmanuals.com/professional/clinical-pharmacology/pharmacokinetics/drug-distribution-to-tissues (Accessed on 26 March 2017).
61. Wang L, Tang L, Zheng Y et al. Determination of bosutinib in mice plasma and tissue by UPLC-MS/MS and its application to the pharmacokinetic and tissue distribution study. *Anal. Methods.* 7(21), 9184-9189 (2015).
62. Mittal G, Carswell H, Brett R, Currie S, Kumar MN. Development and evaluation of polymer nanoparticles for oral delivery of estradiol to rat brain in a model of Alzheimer's pathology. *J. Control. Release.* 150(2), 220-228 (2011).

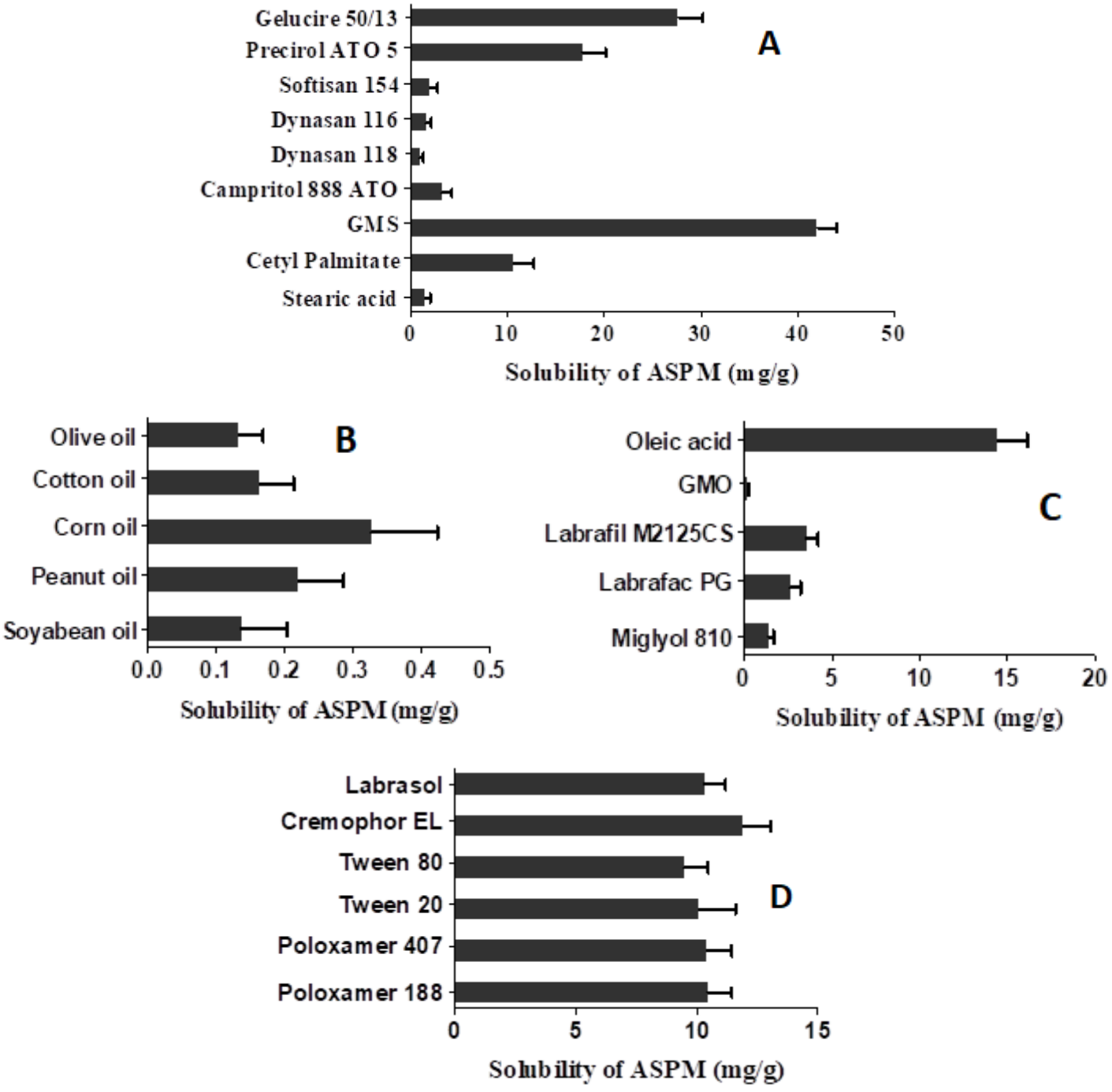

Fig. 1. Solubility study of ASPM

(A) Solid lipids
(B) Vegetable oils
(C) Synthetic oils
(D) 1% w/v surfactant solution
The values are presented as Mean±SD, n=3

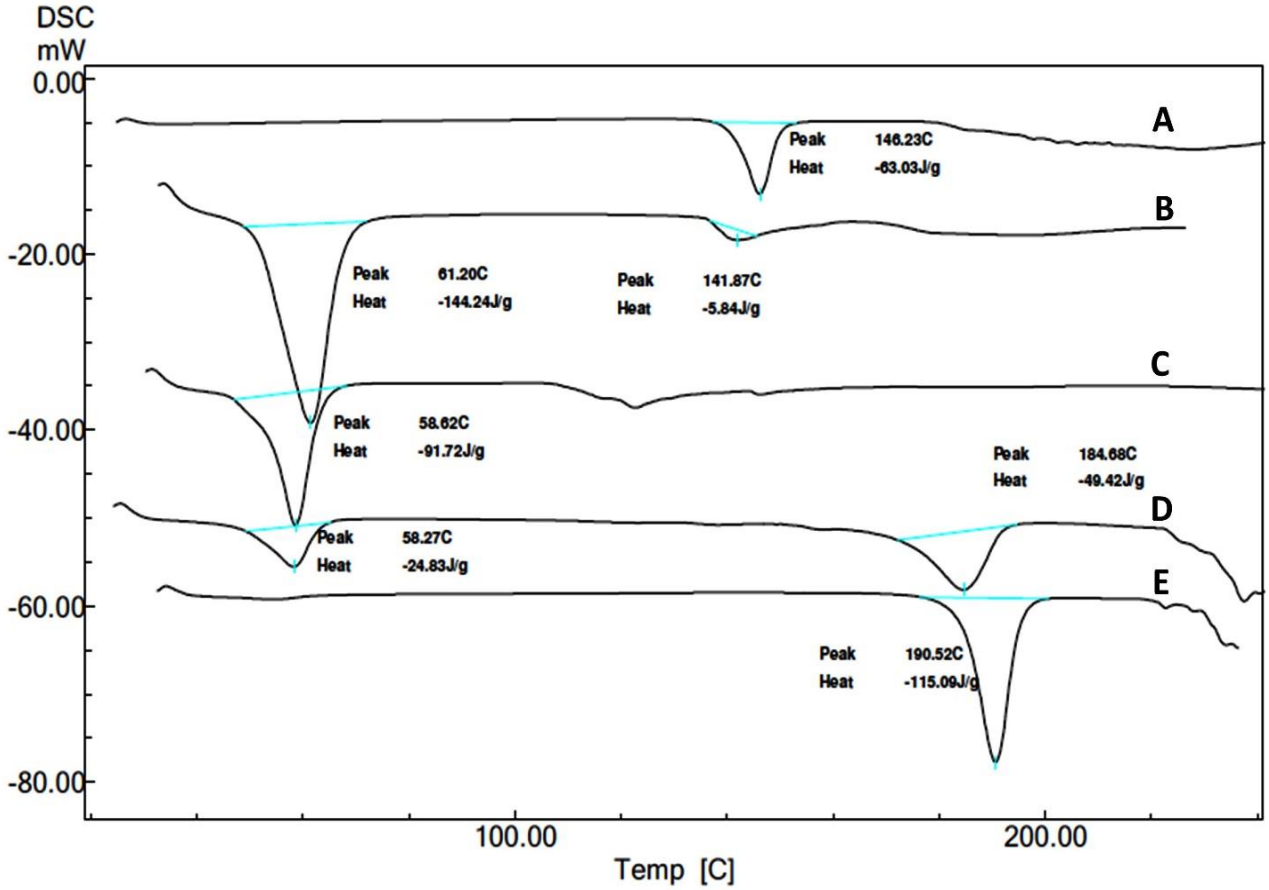

Fig. 2. DSC thermograms

(A) Asenapine maleate (ASPM)
(B) ASPM-GMS physical mixture
(C) ASPM/GMS solid mixture obtained during lipid screening study
(D) ASPM-NLCs containing drug
(E) Sucrose

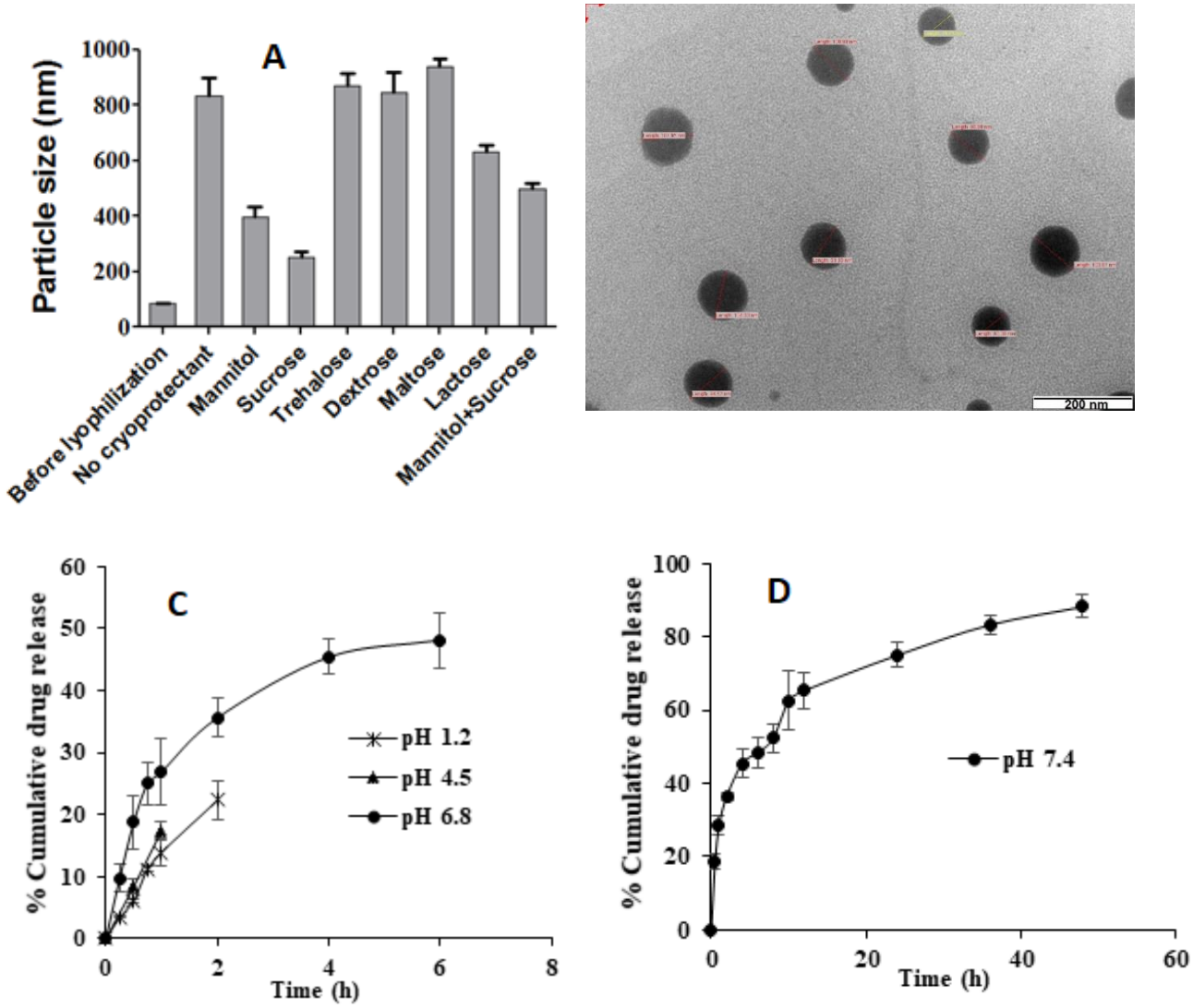

Fig. 3. Assessment of different parameters for NLCs

(A). Particle size of NLCs loaded with ASPM which was lyophilized with different cryoprotectants at concentration of 5% w/v (Mean ± SD, n=3).

(B) Transmission electron micrographs of optimized ASPM-NLCs formulation

(C) *In vitro* dug release data obtained in pH 1.2 HCl buffer, pH 4.5 acetate buffer and pH 6.8 phosphate buffer (Mean ± SD, n=3)

(D) *In vitro* drug release data obtained in pH 7.4 phosphate buffer (Mean ± SD, n=3).

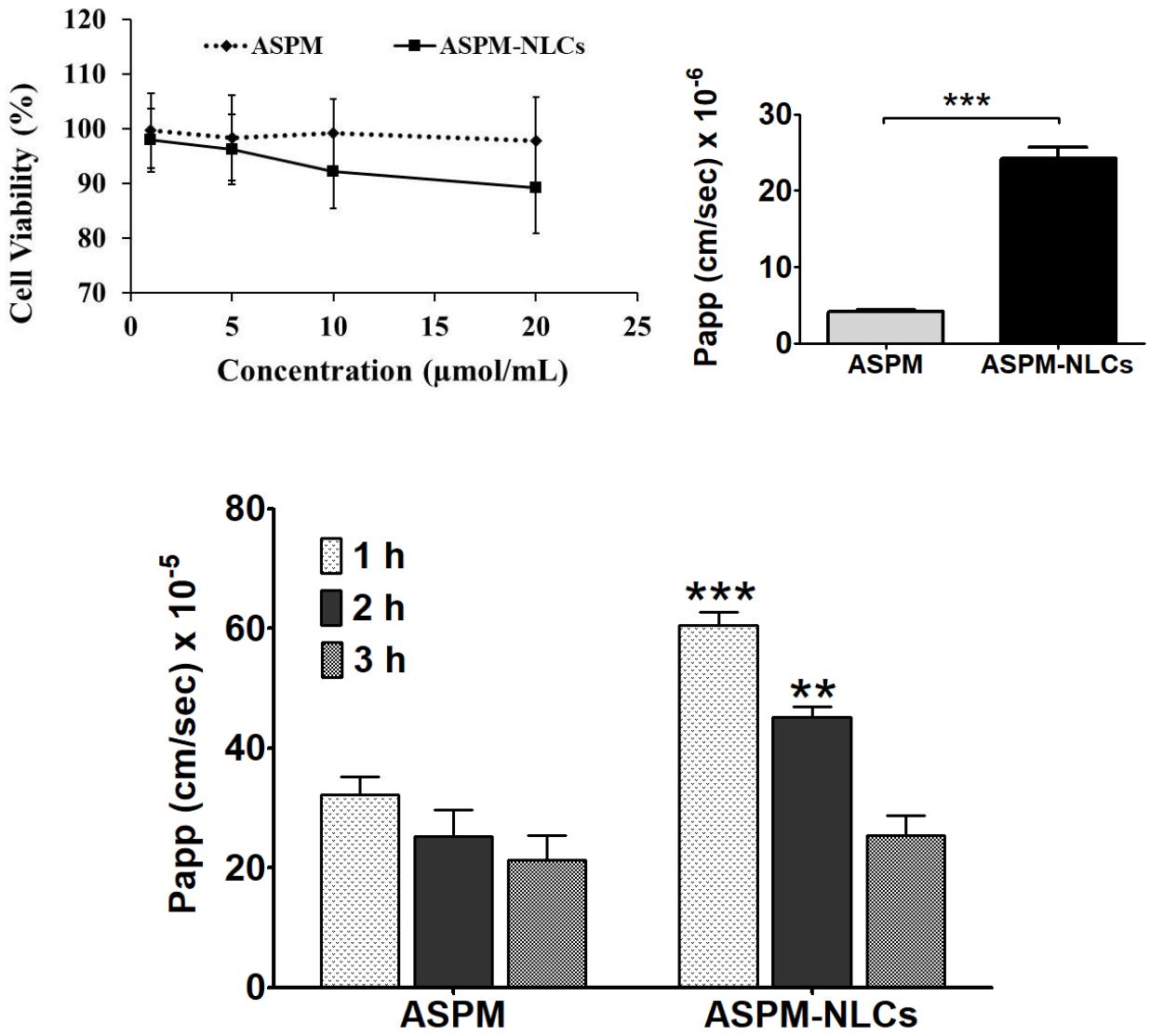

Fig. 4. Cell viability, cell permeability and ex vivo everted rat ileum sac studies.
(A) Cell viability study performed using MTT assay (Mean ± SD, n=6), (B) Cell line permeability study carried out for plain drug and ASPM-NLCs in Caco2 cell line. Results are expressed as apparent permeability coefficient (*P*app) in cm/sec (Mean ± SD, n=6). (C) Ex vivo everted rat ileum sac study to assess the permeability of plain drug and ASPM-NLCs across rat ileum. Results are expressed as apparent permeability coefficient (*P*app) in cm/sec (Mean ± SD, n=4); ***$p < 0.001$ and ** $p < 0.01$.

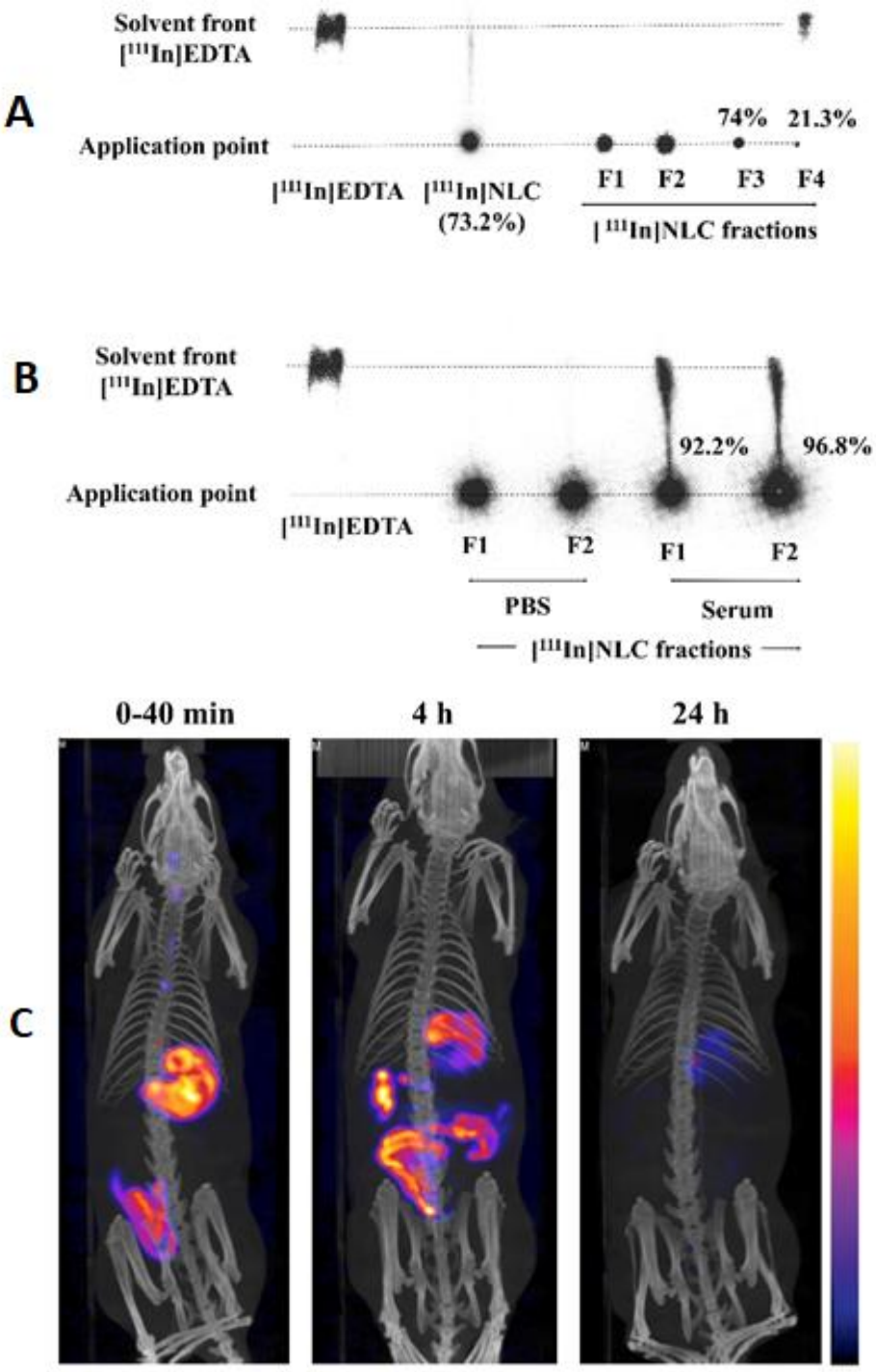

Fig. 5. Radiolabelling and imaging studies.
(A) Radiolabelling efficiency of NLCs with Indium (^{111}In). Thin layer chromatography (TLC) of the [^{111}In]NLCs immediately after radiolabelling and TLC of column fractions of radiolabelled NLCs. **(B) TLC of purified radiolabelled NLCs after incubation with both phosphate buffer saline (PBS) and fetal bovine serum (FBS) for 24 h at 37 °C (C) SPECT/CT images of [^{111}In]NLCs administered rats at 0-40 min, 4 h and 24 h post oral administration ([^{111}In]NLCs (10.2 µmole lipid, 24 MBq).**

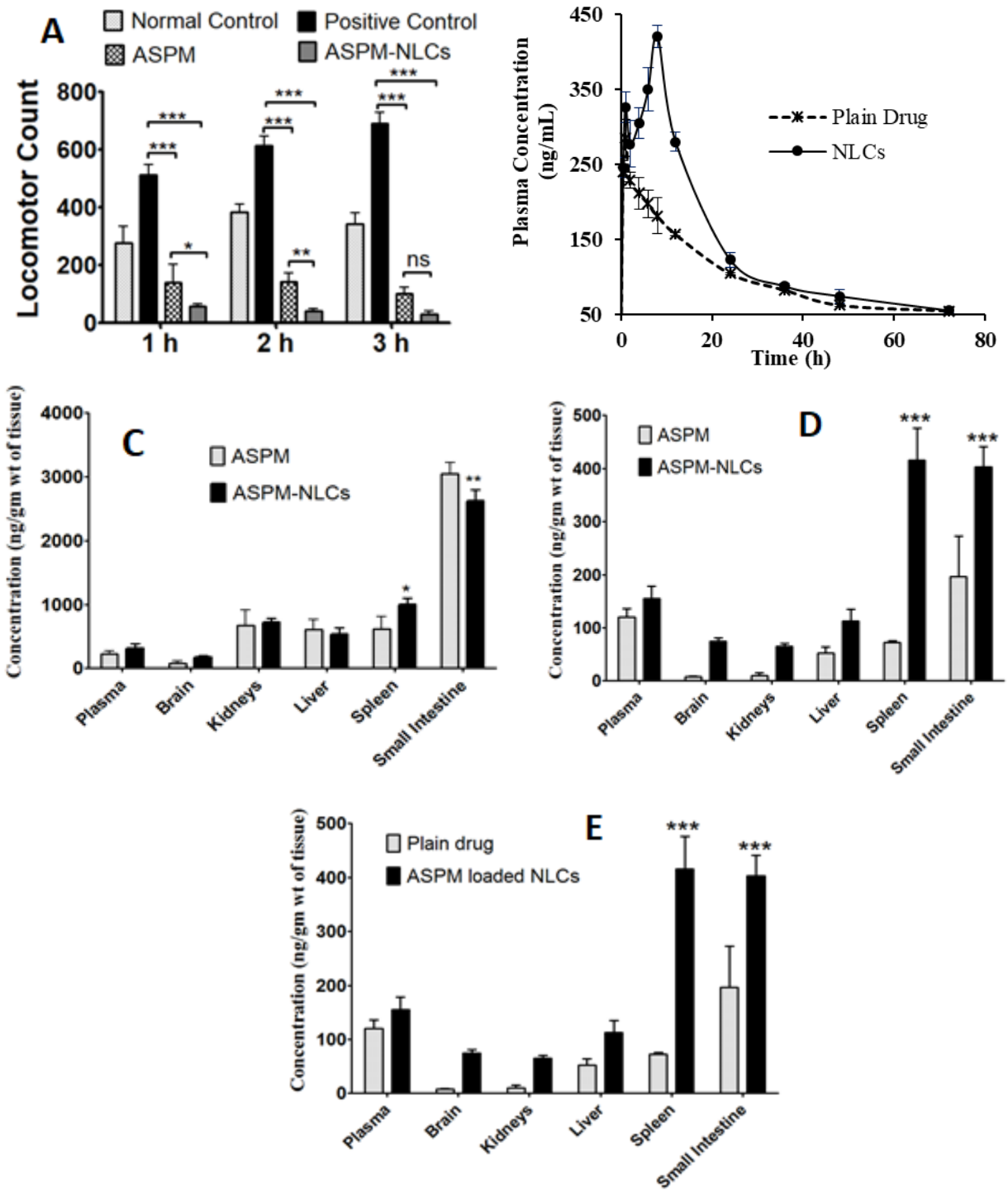

Fig. 6. Efficacy study, pharmacokinetics and tissue distribution studies

A) Locomotor count of ASPM and ASPM-NLCs in different group of rats (Mean ± SD, n=6).
B) Plasma concentration *vs.* time profile obtained in pharmacokinetic study (Mean ± SD, n=6).
C) Tissue distribution for plain drug and ASPM-NLCs at 1 h (Mean ± SD, n=3).
D) Tissue distribution for plain drug and ASPM-NLCs at 8 h (Mean ± SD, n=3).
E) Tissue distribution for plain drug and ASPM-NLCs at 24 h (Mean ± SD, n=3).
*** $p < 0.001$, ** $p < 0.01$, * $p < 0.05$ and ns= no significant

Table 1. Variables with the assigned values at different levels in the Placket-Burman design and Box-Behnken design

Plackett–Burman design		
Factors	**Level**	
	Level-1	**Level-2**
Total lipid (% w/v)	1	2
Surfactant concentration (% w/v)	1	2
Oil content (% wrt total lipid)	10	30
Lipid: Drug ratio	10	30
Sonication amplitude (%)	40	80
Sonication pulse (s)	3	9
Temperature (ºC)	70	90
Sonication time (min)	5	15

Box-Behnken design			
Factors	**Levels**		
	Low (-1)	**Middle (0)**	**High (+1)**
Total lipid (% w/v)	1	1.5	2
Surfactant concentration (% w/v)	1	1.5	2
Oil content (% wrt total lipid)	10	20	30
Lipid: Drug ratio	10	20	30

Table 2. Predicted and observed values for responses with % relative error in Box-behnken design

Response	Predicted Mean ± SD	Predicted 95% PI	Observed Mean ± SD (n=3)	% Relative error
Size (nm)	84.09 ± 14.57	50.65 to 117.52	84.91 ± 2.14	1.0
PDI	0.205 ± 0.047	0.101 to 0.309	0.222 ± 0.026	8.1
ZP (mV)	-4.35 ± 3.67	-12.35 to 3.65	-4.83 ± 0.29	11.0
EE (%)	89.5 ± 1.9	85.3 to 93.7	86.9 ± 1.8	2.9

PDI= Polydispersity index, ZP= Zeta Potential, EE= Entrapment efficiency, PI= Prediction interval

Table 3. The pharmacokinetic parameters of ASPM and ASPM-NLCs when administered orally in rats.

Parameters	**ASPM**	**ASPM-NLCs**
Cmax (ng/mL)	284.93±14.20	420.43±14.50 ***
Tmax (h)	1±0	8±0 ***
AUC_{0-t} (h*ng/mL)	7309.06±458.23	10101.74±683.23 ***
$AUC_{0-\infty}$ (h*ng/mL)	9792.10±356.82	14404.87±1024.65 ***
$t_{1/2}$ (h)	31.6±2.1	54.3±0.6 ***
Vd (mL)	18423.08±1875.70	21526.69±1280.09 **
CL (mL/h)	403.74±14.70	275.14±19.6 ***
Ke (1/h)	0.0220±0.0015	0.0128±0.0002 ***
MRT (h)	26.2±0.7	22.7±0.2 ***

All values are presented as Mean±SD, n=6; Ke= Elimination rate constant; $t_{1/2}$= Elimination half-life; AUC= Area under the curve; Vd= volume of distribution; CL= Clearance; MRT= Mean residential time. *** $p< 0.001$ and ** $p< 0.01$.